2.A.1 *Nuclear Physics* **A164** (1971) 1—10; © *North-Holland Publishing Co., Amsterdam*
Not to be reproduced by photoprint or microfilm without written permission from the publisher

LOW-ENERGY CROSS SECTIONS FOR ^{7}Li(p, α)^{4}He AND ^{6}Li(p, α)^{3}He

H. SPINKA and T. TOMBRELLO
California Institute of Technology †
and
H. WINKLER
California State College, Los Angeles †

Received 12 January 1971

Abstract: Reaction cross sections for ^{6}Li(p, α)^{3}He and ^{7}Li(p, α)^{4}He were obtained using lithium beams and a CH_4 gas target at equivalent proton energies between 130 keV and 560 keV. The Rutherford scattering of lithium on carbon was used as a cross-section standard. For ^{6}Li+p, an extrapolation of the cross section to the energy region of astrophysical interest is given.

E NUCLEAR REACTIONS ^{6}Li(p, α), E = 151, 317 keV; ^{7}Li(p, α), E = 130, 271, 416, 561 keV; measured $\sigma(\theta)$; deduced σ_t.

1. Introduction

The reactions ^{7}Li(p, α)^{4}He and ^{6}Li(p, α)^{3}He are both of significant astrophysical interest. The ^{7}Li+p reaction occurs as a final step in the fusion cycle that converts hydrogen to helium. In the sun this reaction is estimated to account for 9 % of the terminations of the p-p chain, which is the major solar energy source. Both reactions are also important because they have large cross sections for the destruction of lithium isotopes and thus may fundamentally affect the universal abundance of lithium. It seems likely that both will play significant roles as secondary reactions in controlled fusion processes. In particular, ^{6}Li(p, α)^{3}He yields a ^{3}He nucleus that may be "reused".

Total reaction cross sections for ^{6}Li(p, α)^{3}He and ^{7}Li(p, α)^{4}He have been measured by several authors in the energy range from E_p = 20 keV up to several MeV. A fairly complete survey of all results up to E_p = 1 MeV has recently been made by Audouze and Reeves [1]) for astrophysical purposes. The experimental results disagree at certain energies by up to a factor of 3, usually outside the quoted errors. Audouze and Reeves have tried to improve this situation by re-normalizing certain sets of data, but the result can hardly be considered satisfactory.

All cross-section measurements on ^{6}Li(p, α)^{3}He and ^{7}Li(p, α)^{4}He performed up to now have used solid lithium targets. The cross-section values were obtained from

† Supported in part by the National Science Foundation (GP-9114 and GP-19887).

beam current integration, measured counter solid angles and thickness and composition of the target. However, lithium reacts very quickly with the contaminants nitrogen and oxygen, producing a poorly defined target composition, and time-dependent yields from lithium targets have been reported frequently in the literature. In some work results have been obtained for different target thicknesses and then extrapolated to zero thickness. For ^{6}Li+p in the energy range E_p = 50 to 190 keV, Gemeinhardt *et al.* [2]) have combined this method with a flame spectroscopic determination of the amount of lithium in the target, thereby avoiding the problem of contaminants. The elastic scattering of protons from lithium as determined by McCray [3]) has also been used as a cross-section standard. However, these elastic scattering measurements are subject to the same contamination problems since they also involved a lithium target.

The work described here uses a method of absolute cross-section determination which completely avoids the difficulties with lithium targets. An isotopically pure lithium beam is used to bombard protons in a differentially pumped gas target. The gas contains the hydrogen bound in a well-defined stoichiometric ratio to a much heavier element, in our case carbon. The pure Rutherford scattering of lithium on carbon is observed and used as a cross-section standard. We then obtain the reaction cross section from the ratio of number of counts in two particle groups. No beam integration is necessary. The target gas pressure and the mean charge state of the lithium beam enter only into the calculation of the true beam energy in the target region.

Angular distributions and total cross sections were measured at equivalent proton energies of E_p = 151 and 317 keV for ^{6}Li+p, and E_p = 130, 271, 416 and 561 keV for ^{7}Li+p. The results obtained are believed to be free from uncontrolled systematic errors. For ^{6}Li+p a cross-section extrapolation down to energies of astrophysical interest is made by combining our results with the data of Gemeinhardt *et al.* [2]). No such extrapolation is possible from our results on ^{7}Li+p, because of the presence of resonances in the compound nucleus ^{8}Be.

2. Experiment

Negative ion beams of ^{6}Li and ^{7}Li were obtained from the exchange canal of a negative helium ion source. Hydrogen gas was used in the duoplasmatron source to provide the ionizing beam. After acceleration in the ONR-CIT tandem accelerator, singly charged lithium beams of typically 0.1 μA were obtained at the target. Some difficulties were experienced at the lowest bombarding energy, 1 MeV, and it was necessary to reduce the tank pressure at this point in order to obtain proper operation of the corona stabilizer.

The target, shown in fig. 1, is differentially pumped in two stages. The first stage consists of an 85 l/sec Roots pump (Heraeus WS 250); the second stage is pumped by a

are given in the figure. The second canal, between the Roots pump and diffusion pump, has collimators of 2.5 mm diameter on both ends and restricts the beam geometrically. The canal before the target region is much wider and threaded on the inside in order to minimize scattering of the beam. At a target pressure of 3.0 Torr, the gas consumption was about 25 l of CH_4 per hour (at STP), with over 98 % of this flowing through the Roots pump.

In our method of cross-section measurement, beam integration is not necessary and was not attempted. In order to maximize the beam in the target chamber and to monitor the beam current, a 5 cm diameter photomultiplier was mounted between the target chamber and the beam stop, the cathode facing the beam. The light produced

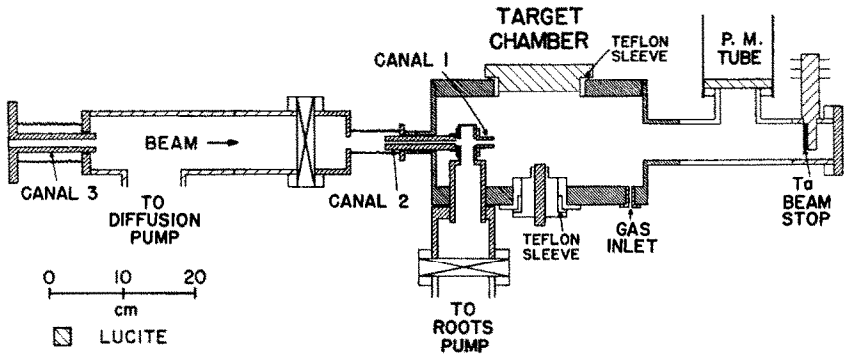

Fig. 1. Differentially pumped gas target. The dimensions of the canals are: canal 1, 0.5 cm diameter, 2.5 cm long; canal 2, 0.35 cm diameter, 10 cm long.

in the gas by as little as 1 nA of beam current was easily detected in the photomultiplier output current. Since the reaction products have to be measured at many different angles and their number is orders of magnitude below that of the elastically scattered particles, it is not practical to measure both in the same counter. Knowing the angular distribution of Rutherford scattering it is sufficient to measure the elastic scattering at one angle and the ratio of geometrical factors (Ωl) (l = length of target region) of two counters. The latter is measured using Rutherford scattering again, as described later. Three movable counters and a fixed counter at $\theta = 90°$ were used in the experiment. One of the movable counters was strongly collimated ($\Delta\theta = \pm 0.7°$) and detected the elastic scattering of the beam particles from carbon as well as the elastic carbon and hydrogen recoils. Before the actual experiment this counter was set as close as possible to the angle of $\theta = 45.0$. A carbon beam was used to find the peak yield position for the 45° lab Mott elastic scattering peak of carbon on carbon. The correct counter setting was always found within $\pm 0.3°$ of the protractor 45.0° reading, as aligned with a telescope. In our method, the angle error of the counter for the elastic scattering enters rather strongly into the final error of the reaction cross section.

The elastically scattered beam particles and the carbon and hydrogen recoils were always well separated in the spectra obtained with the 45° counter. Even at the highest bombarding energy the 45° elastic scattering cross section of lithium from carbon is very large compared to the Li + p reaction cross sections. Therefore, the elastic spectra were in no way distorted by the few reaction particles entering this counter.

The angular openings of the movable counters for the reaction products were $\Delta\theta = \pm 5.5°$ and $\Delta\theta = \pm 5°$, respectively. Measurements with these counters were carried out for lab angles between 20° and 147°. The fixed counter had an angular

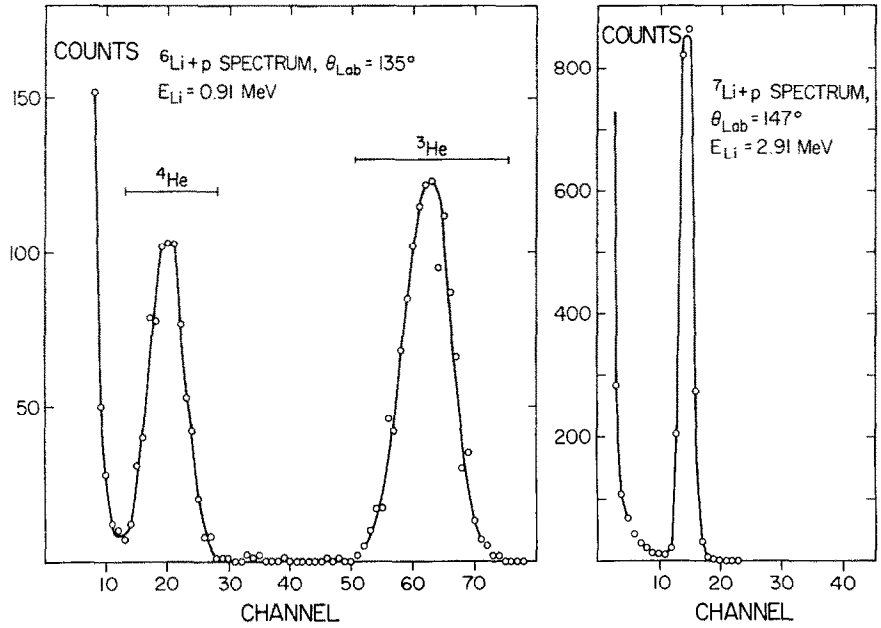

Fig. 2. Backward counter charged particle spectra. These are not typical spectra, but are from the most critical region where low-energy α-particles were counted. The counter was covered with a foil thick enough to stop all elastically scattered Li particles.

opening of $\Delta\theta = \pm 11°$. All three reaction product counters were completely protected from elastically scattered particles or recoils by foils. Foils of thickness 0.9 and 3.4 mg/cm^2 were used in the forward counter and 0.22 and 1.4 mg/cm^2 in the backward counter, for ^{6}Li and ^{7}Li, respectively. For the ^{6}Li + p reaction, the ^{3}He and ^{4}He particles were always completely separated at forward angles. Separation was also good at 1 MeV for the 90° counter. At backward angles and 1 MeV bombarding energy the ^{4}He was too low in energy to be observed beyond 140°. The spectrum of the backward counter for this ^{6}Li energy and $\theta_{lab} = 135°$ is shown in fig. 2. For a ^{6}Li energy of 2 MeV the ^{4}He energy was too low to be observed beyond 90°. The ^{7}Li + p reaction has a larger Q-value, but the ^{4}He laboratory energy also becomes quite small at backward angles and higher bombarding energies because of the large c.m. motion.

A ^{4}He spectrum from this reaction, at the most backward angle measured, is shown in fig. 2.

The ratio of the geometrical factor $\langle \Omega l \rangle$ of the 45° counter (elastics) to the geometrical factor of each of the two movable reaction product counters was obtained in the following way. The target chamber was filled with high-purity argon and the elastic scattering of 1.8 MeV protons on argon was observed in the different counters.

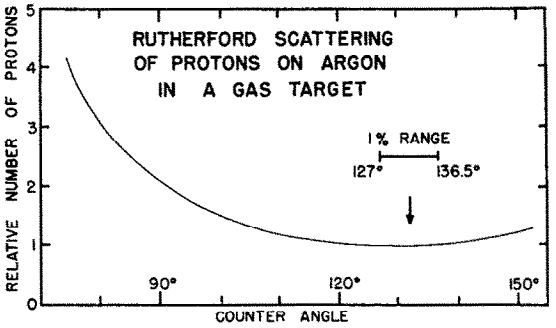

Fig. 3. Count rate as a function of counter angle for the Rutherford scattering of protons on argon in a gas target.

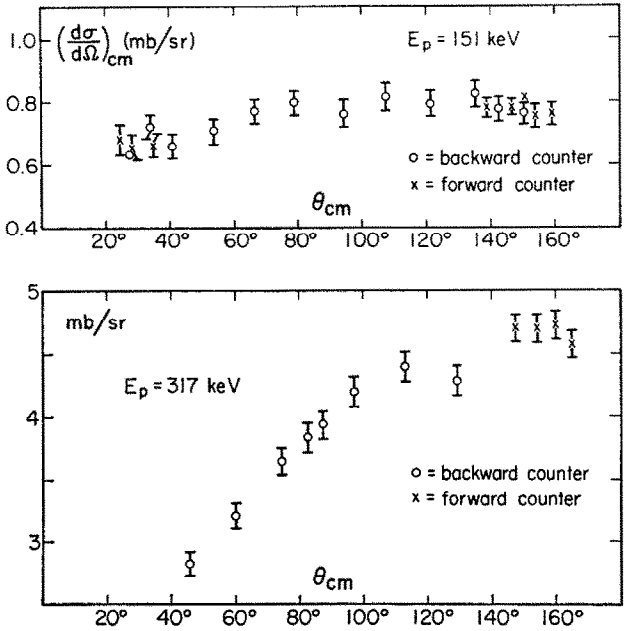

Fig. 4. Differential cross sections for ^{6}Li(p, α)^{3}He. The $\theta_{c.m.}$ is the angle of the ^{3}He in the c.m. system. Note the suppressed zeroes on the cross-section scales. Some points were obtained by reflecting ^{4}He measurements. Points from forward and backward counters are given separately to show the good agreement. The errors given do not include an uncertainty of about ±8 % from the absolute normalization of the cross sections to Rutherford scattering.

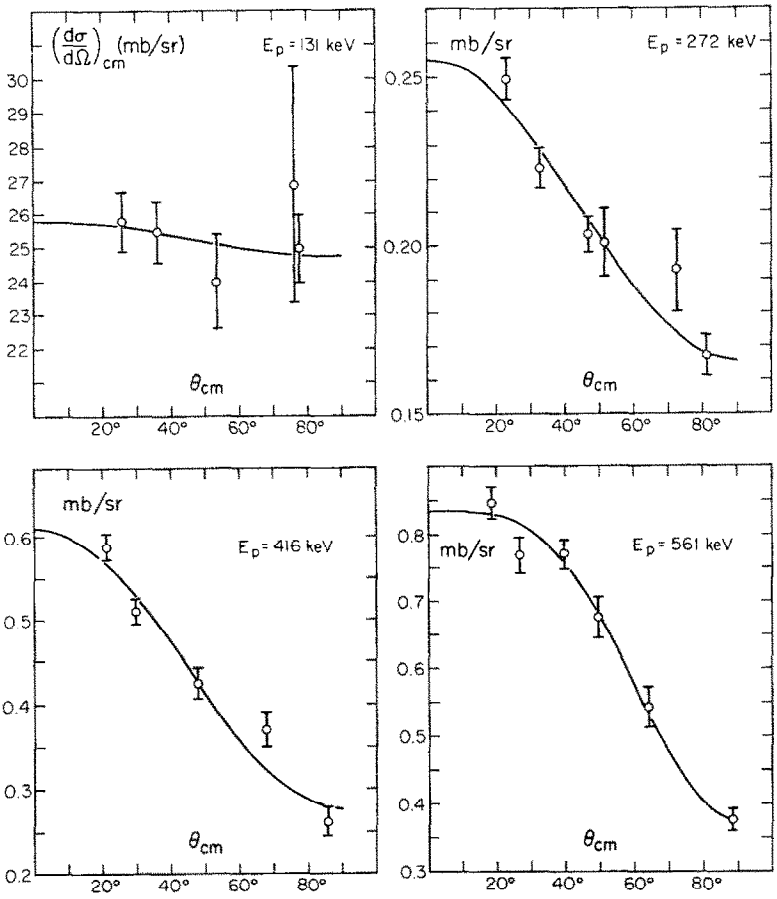

Fig. 5. Differential cross sections for ^{7}Li(p, α)^{4}He. The $\theta_{c.m.}$ is the angle of ^{4}He in the c.m. system. Note the suppressed zeroes on the cross-section scales. Some points were obtained from measurements in the backward hemisphere using the symmetry of the angular distributions about $\theta_{c.m.} = 90°$. Legendre polynomials of order 0 and 2 were used to fit the data of the three lowest energies. The $E_p = 561$ keV data were fit with orders 0, 2 and 4. These least-square fits, shown in the figure, were used to obtain the total reaction cross section.

At $E_p = 1.8$ MeV the elastic scattering of protons [4, 5]) on argon follows strictly the Rutherford expression to at least 140°. In the observation of a differential scattering cross section proportional to $[1/\sin \frac{1}{2}\theta_{c.m.}]^4$ in a gas target, a relative minimum in the count rate occurs at a certain backward angle. If a collimated counter is moved in the direction of increasing backward angle, the decrease in count rate resulting from the decreasing $d\sigma/d\Omega$ is compensated by the increase in the length of the target as seen by the counter [6]). For an infinitely heavy scatterer, the minimum occurs at $\text{tg}\, \frac{1}{2}\theta = \sqrt{5}$, $\theta = 132°$. A calculated curve for the ^{40}A + p case is shown in fig. 3. The minimum is fairly broad; the background was never larger than 5 % and the largest estimated error

due to incorrect background subtraction is 2 % of the total number of counts in a line. Since all angular distributions contain points obtained with different counters, a small (±2 %) uncertainty in the determination of the geometrical factor of each counter relative to the elastics counter was also taken into account. No corrections were made, or errors assigned, for the effect of the finite angular openings of the counters. The values of $d\sigma/d\Omega$ given in figs. 4 and 5 do not include the uncertainty (approximately ±8 %) that results from the normalization of the cross section to the elastic scattering.

TABLE 1

Total reaction cross-section results

	Li bombarding energy (MeV)	E_p (keV) [a])	σ_{total} [b]) (mb)
^{6}Li(p, α)^{3}He	0.907	151.0±3.5	9.8 ±1.0
	1.903	317.0±4.0	47 ±5
^{7}Li(p, α)^{4}He	0.913	130.5±3.5	0.32±0.04
	1.899	271.5±4.0	2.46±0.25
	2.913	416.0±3.5	4.9 ±0.5
	3.925	561.0±3.0	7.4 ±0.8

[a]) Equivalent proton bombarding energy as calculated from the lithium bombarding energy, the beam energy losses and the masses of Li and H.

[b]) The error given is the estimated total uncertainty in the absolute value of the cross section from all error sources.

For ^{6}Li+p the total cross sections were obtained by multiplying the measured points with $2\pi \sin\theta$. A smooth curve through these values was then numerically integrated. The ^{7}Li+p total cross sections were obtained by fitting the data with either 2 or 3 even order Legendre polynomials. The fits are shown in fig. 5. Table 1 gives the total cross sections.

A number of possible sources of errors affecting the absolute cross-section determinations were considered. These are:

(i) Changes in the stoichiometric ratio of carbon to hydrogen in the target gas due to dissociation by the beam, followed by condensation of free carbon. Several different calculations have shown this to be a very small effect that can be completely neglected. Even under the assumption that all the energy lost by the beam goes into the splitting of CH_4 molecules and all free carbon immediately disappears from the target region, the high gas flow and low beam current hold the number of split molecules several orders of magnitude below 1 % of the total number of molecules present. Since the target gas was methane with a purity of better than 99.9 %, an exact C to H ratio of 1 : 4 was assumed with no error assigned.

(ii) Angular position of the elastics counter. For Rutherford scattering of lithium on carbon at 45°, a change of 1° in angle changes the lab differential scattering cross

section by 9 %. An angle error of $\pm 0.5°$ was assumed for this counter, based on several alignments at 45° using the peak in the Mott scattering of carbon on carbon, as described before. In spite of the rapid variation of σ_{elastic} with angle, a correction for the small but finite θ angular opening of the elastic counter is not necessary.

(iii) Energy of the beam in the target region. This affects not only the energy at which the total cross section is measured but also the value of the elastic cross section used in the data evaluation. For the worst case, 1 MeV bombarding energy, an error of ± 5 % in the elastic cross section was calculated, based on considerations of the possible amount of gas to be traversed by the beam and uncertainties in the mean charge state [7]) and energy loss data [8]).

(iv) The ratio of the geometrical factors $\langle \Omega l \rangle$ of a reaction particle counter and the elastics counter. A small error from the statistics of this determination was already taken into account at each point of the angular distribution.

(v) Integration of the measured angular distribution. This error contains effects from the error of individual points in the angular distribution, as well as from the quality of the fits and the uncertainties in the contributions of the regions near 0° and 180°, not measured in our experiment. All independent errors of the total cross-section determination were added quadratically; the resulting final errors are given in table 1.

3. Conclusions

The ^{7}Li *nucleus.* Our cross section at $E_p = 130$ keV agrees with an interpolation between the values of Sawyer and Phillips [9]) at 120 and 140 keV, within the large error (± 25 %) of their measurements. At the three higher energies our results agree fairly well with, but are always higher than, the cross sections derived for this energy range by Audouze and Reeves [1]). These authors normalized a yield curve obtained by Conrad *et al.* [10]) for $E = 150$ of 600 keV to a yield curve of Haeberli (unpublished) for $E_p = 0.4$ to 3.4 MeV. Haeberli's results in turn had been normalized in ref. [1]) to the absolute cross-section measurements of Mani *et al.* [11]) between $E_p = 1$ and 3.4 MeV. A fairly large error of typically ± 20 % was estimated in ref. [1]) for the cross sections derived by the re-normalizations. (Unfortunately, the figure published in ref. [1]) for the $S(E)$ values derived from these cross sections contains some misprints.) It is not possible to use our results for an extrapolation of the cross section down to energies of astrophysical interest, because of the presence of resonances in the compound nucleus ^{8}Be. Reliable cross-section measurements at lower energies would be needed for such an extrapolation.

The ^{6}Li *nucleus.* There is a considerable amount of scatter in the earlier data for ^{6}Li(p, α)^{3}He even after re-normalization, as can be seen from fig. 1 of the Audouze and Reeves paper. At $E_p = 150$ keV both our angular distribution and total cross section agree very well with the results of Gemeinhardt *et al.* [2]). On the other hand, interpolation of Sawyer and Phillip's results [9]) at $E_p = 140$ and 160 keV

leads to a total cross section almost twice our result. Our value at $E_p = 317$ keV is 12 % higher than Bertrand's [12]) with the two errors overlapping. Our angular distributions at both energies are also in agreement with the work of Beaumevieille *et al.* [13,14]). However, the total cross section derived by Audouze and Reeves from Beaumevieille's work by normalization to McCray's [3]) data at $E_p = 600$ keV is about 30 % lower than our value at $E_p = 317$ keV, clearly outside the combined errors.

Since the work of Gemeinhardt *et al.* seems to be the most careful and comprehensive experiment on the ^{6}Li(p, α)^{3}He low-energy cross section, we have used their results together with our data for a cross-section extrapolation to energies of astro-

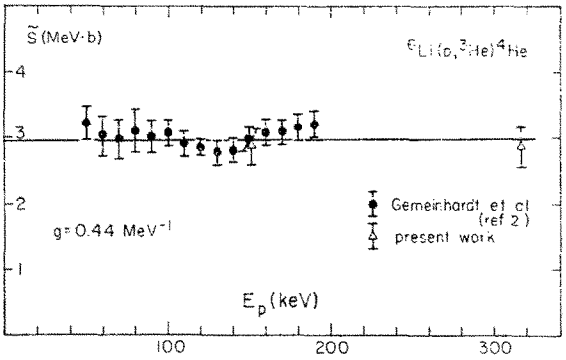

Fig. 6. The cross section factor $\tilde{S}(E)$ as derived from

$$\sigma_{tot} = \frac{\tilde{S}(E)}{E} \exp\left(-\frac{2.758}{\sqrt{E}} - gE\right),$$

where E is the c.m. energy in MeV and $g = 0.44$ MeV^{-1} (see text). The low-energy values are from measurements of Gemeinhardt *et al.* [2]), σ_{tot} varies by a factor of 400 over the energy range covered by the experimental points given. From the quality of the fit of $\tilde{S}(E) =$ constant to the data, it would seem that the errors of the experimental points are over-estimated. However, the errors given contain contributions from the absolute cross-section determination which are only weakly dependent on E_p.

physical interest. Our combined data cover the energy region from $E_p = 50$ to 317 keV with a variation in the cross section of a factor of 400. No re-normalization of any kind was used.

For this low-energy region well below the Coulomb barrier and with only s-wave protons participating in the reaction, the cross section can be written as:

$$\sigma_{tot} = \frac{\tilde{S}(E)}{E} \exp\left(-2\pi\eta - gE\right).$$

This is the first-order expression for the barrier penetration, with

$$\eta = \frac{Z_1 Z_2 e^2}{\hbar v} = \frac{2.758}{\sqrt{E}}, \quad g = 0.122\left(\frac{AR^3}{Z_1 Z_2}\right)^{\frac{1}{2}}, \quad A = \frac{A_1 A_2}{A_1 + A_2},$$

$R = r_0(A_1^{\frac{1}{3}} + A_2^{\frac{1}{3}}) =$ square well radius in fm,

where indices 1 and 2 indicate the proton and ^{6}Li, respectively; and all proton energies are in MeV in the c.m. system. Taking $r_0 = 1.3$ fm one obtains $g = 0.44\ \mathrm{MeV}^{-1}$. The σ_{tot} value is then used to calculate $\tilde{S}(E)$. The result is shown in fig. 6, where the errors of σ_{tot} are plotted as errors in $\tilde{S}(E)$ and a straight line was used to make a least-squares fit to the data. The slope of $\tilde{S}(E)$ was found to be zero within the errors, and $\tilde{S}(0) = 3.0\ \mathrm{MeV} \cdot \mathrm{b}$. At proton energies below 10 keV, the cross-section values obtained from our expression are about 25 % higher than the values obtained in ref. [1]).

References

1) J. Audouze and H. Reeves, Astrophys. J. **158** (1969) 419;
Contribution de l'I.A.P. Paris (Institut d'Astrophysique) (1969) unpublished report
2) W. Gemeinhardt, D. Kamke and C. von Rhöneck. Z. Phys. **197** (1966) 58
3) J. A. McCray, Phys. Rev. **130** (1963) 2034
4) J. Cohen-Ganouna, M. Lambert and J. Schmouker, Nucl. Phys. **40** (1963) 82
5) G. A. Keyworth, G. C. Kyket, Jr., E. G. Bilpuch and H. W. Newson, Phys. Lett. **20** (1966) 281
6) M. R. Dwarakanath, Ph.D. thesis, California Institute of Technology (1968)
7) C. S. Zaidins in Nuclear reaction analysis tables (North-Holland, Amsterdam, 1968)
8) W. Whaling, Handbuch der Physik, vol. 34 (Springer Verlag, Berlin, 1958) p. 193
9) G. A. Sawyer and J. A. Phillips, unpublished Los Alamos report L.A. 1578 (1953)
10) B. Conrad, V. Konih and U. Timm, Nature **45** (1958) 205
11) G. S. Mani, R. Freeman, F. Picard, A. Sadighi and D. Redon, Nucl. Phys. **60** (1964) 588;
J. M. F. Jeronymo, G. S. Mani and A. Sadighi, Nucl. Phys. **43** (1963) 424
12) F. Bertrand, G. Grenier and J. Pornet, unpublished C.E.A. report R. 3428 (C.E.A. Saclay), 1968
13) H. Beaumevieille, A. Longequeue and J. P. Longequeue, Compt. Rend. **256** (1963) 1494
14) H. Beaumevieille, unpublished C.E.A. report R. 2624 (1964)